J Mater Sci (2012) 47:1011–1017
DOI 10.1007/s10853-011-5881-1

The influence of nano-silica on the hydration of ordinary Portland cement

G. Land · D. Stephan

Received: 27 April 2011 / Accepted: 17 August 2011 / Published online: 7 September 2011

Abstract Nucleation seeding is a new approach to control the kinetics of cement hydration. It is known that nano-silica has an accelerating effect on cement hydration. It is assumed that the surface of these particles act as a nucleation site for C–S–H-seeds which then accelerate the cement hydration. In this case the acceleration should depend on the particles surface area. To verify this, nano-silica particles of different sizes and specific surface areas were synthesised. The acceleration of cement hydration clearly correlates with the total surface size of the added particles, which was varied by either using smaller particles or higher concentration of particles in the cement lime. Additional in situ-XRD experiments show that the consumption of C_3S and the formation of portlandite are accelerated by the addition of nano-silica. In both cases the surface size is the major factor for the hydration kinetics.

Introduction

Silica fume is a widely-used material to enhance the performance of construction materials today. The particle size in silica fume ranges from a few nanometres to the micrometre scale as shown in Fig. 2. One of the first true nanomaterials used in cementitious materials was colloidal silica. In contrast to silica fume the particle size can be adjusted very precise during production. A large variety of methods to produce nano-silica are known today [1, 2]. Sol–gel processes like the well-known Stöber-process [3] have a high reproducibility and offer a number of ways to control the final particle size [4–7]. Silica sols produced by sol–gel processes based on sodium silicate are used in huge quantities in different industrial sectors [2, 8]. The pyrogenic route is also used to produce high amounts of so-called fumed silica or aerosol [2, 9]. Furthermore other production methods like the precipitation from olivine in sulphuric acid [8, 9] and the digest of California red worms humus [10] are known.

The aim of the application of ultra-fine additives like nano-silica in cementitious systems is to improve the characteristics of the plastic and hardened material. Micro- and nano-scaled silica particles have a filler effect by filling up the voids between the cement grains. With the right composition, the higher packing density results in a lower water demand of the mixture and it also contributes to strength enhancement due to the reduced capillary porosity. Beside this physical effect nano-silica has a pozzolanic reactivity which is much higher compared to silica fume [11]. Both effects are very important for the formulation and performance of ultra-high performance concrete (UHPC) [12–15]. The pozzolanic reactivity of quartz powder depends on the particle size due to the high surface to volume ratio of ultra-fine particles [16, 17]. Coarse quartz particles are known to be virtually non-reactive during cement hydration, but the reactivity increases significantly with decreasing particle diameters on the nano scale and nano-silica made by sol–gel processes are expected to show the same characteristics [18].

The pozzolanic reaction of silica with portlandite, which is formed during the hydration of ordinary Portland cement (OPC), produces additional calcium silicate hydrate (C–S–H) which is the main constituent for strength and density in the hardened cement paste. At the same time portlandite,

G. Land · D. Stephan (✉)
Department of Civil Engineering, Building Materials and Construction Chemistry, Technische Universität Berlin, Gustav-Meyer-Allee 25, 13355 Berlin, Germany
e-mail: stephan@tu-berlin.de

which hardly contributes to strength development, is consumed.

Several studies showed that the application of nano-silica in cementitious systems increases the strength development, especially at the early stage of hydration [19–25]. Björnström et al. [26] and Collodetti [27] could show that colloidal silica is an accelerator for cement hydration. Korpa et al. [19] and Ji [28] found the permeability of cement stone to be lower and the microstructure to be more dense when nano-silica is added.

Thomas et al. [29] showed that the hydration of tricalcium silicate (C_3S) can be accelerated by addition of nanoscaled silica or C–S–H-particles. The model that describes these effects assumes that C–S–H-particles are spread in the water between the cement particles and serve as seeds for the formation of C–S–H-phase. Thus the formation of the C–S–H-phase is no longer limited on the grain surface alone, as in the pure C_3S, but also takes place in the pore space. The evasion of time-consuming nucleation processes and the large number of seeds thereby cause an acceleration of C_3S hydration. At the same time the hardened paste should develop less porosity when compared with pure C_3S.

When nano-silica is added to hydrating C_3S the model describes an early pozzolanic reaction on the silica surface to form C–S–H-seeds. These seeds then will act like the pure C–S–H-seeds described above. Figure 1 illustrates the hydration of cement grains without additives (A) compared with the hydration when silica (B) or C–S–H-particles (C) are added. Due to the time that is necessary for nucleation processes the acceleration is not as strong as for the addition of C–S–H-particles, which directly serve as nucleation seeds.

If the accelerations observed by Thomas et al. are based on nucleation processes on the silica surface, there should be a correlation between the size of the total silica surface and the acceleration of C_3S, respectively cement hydration, which is to be examined more exactly in the further study.

Experimental procedure

Nine different silica sols were used in this study. Four of them were supplied by Chemiewerke Bad Köstritz. The samples were precipitated from sodium silicate (water glass) and are labelled based on their average diameter (Köst + diameter). The other ones were synthesised by the Stöber-method. Ethanol (99 vol.%), ammonia (32 wt%, both AppliChem), tetraethyl orthosilicate (TES28, Wacker Chemie) and deionised water were mixed with different quantities to precipitate particles of different size. The compositions of the solutions are shown in Table 1. After 24 h the silica particles were transferred to an aqueous sol by centrifugation and re-dispersion in water. The particle size, size distribution and specific surface area of the Stöber-silica was compared with commercial silica fume (Microsilica Grade 971-U, Elkem Materials, 98% SiO_2).

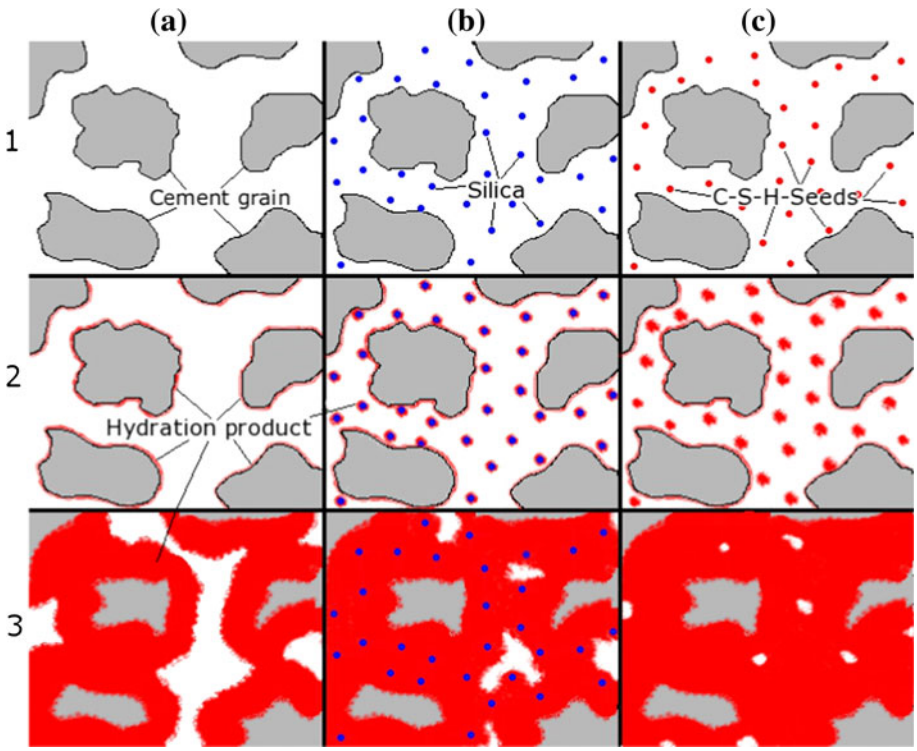

Fig. 1 Hydration process of pure cement (**a**) and with addition of nano-silica (**b**) and C–S–H-seeds at different times (1–3) after mixing

Table 1 Initial composition of solutions for precipitation of silica particles by Stöber-method

Solution	Ethanol, 99 vol.%, mL	Ammonia, 32 wt%, mL	Deionized water, mL	TEOS, mL
1	750	31.7	8.9	33.3
2	750	47.4	13.3	33.3
3	750	29.9	49.1	40.1

White cement of type CEM I 42,5 R (Dyckerhoff Weiss DECOR, Dyckerhoff) was used as an ordinary Portland cement in this study. The white cement was chosen, because of the very low iron content, which is favourable for X-ray diffraction and solid state NMR measurements. An analysis of the cement composition is given in Table 2.

The final particle size was determined by dynamic light scattering using an Nanophox (Sympatec) instrument. The specific surface area of the silica particles was determined on freeze-dried sols by the BET method (Autosorb-1, Quantachrome) using nitrogen gas and on dispersed silica by the Sears method [30] (Titration unit of ZetaProbe, Colloidal Dynamics).

For heat flow calorimetry, 2 g of cement was mixed with a silica sol, which was diluted with deionised water to bring the total water/solid mass ratio to 0.5 and the silica/cement mass ratio to the desired value. Silica/cement mass ratios from 0.01 to 0.1 were investigated. The paste was mixed for two minutes in a sealed plastic ampoule, which was placed into the isothermal calorimeter (TAM Air, Thermometric). The instrument was set to a temperature of 36 °C to get reaction conditions equal to the in situ-XRD experiments. The time resolution was 30 s. All results were ensured by double determinations which were consistent.

The cement paste for X-ray diffraction was mixed in the same way as in the calorimetric experiments. The cement paste was placed in the sample holder of the diffractometer (D4 ENDEAVOR, Bruker AXS with LynxEye detector), sealed with a kapton-foil (Chemplex Industries) and placed in the instrument. It was not possible to cool the sample and a temperature of 36 °C was determined near the sample surface during measurement. With a $\theta/2\theta$-arrangement a range from 5°-65° was measured in 0.02° steps using the Cu k_α-line. For 24 h one diffractogram was taken every 15 min. The single diffractograms were combined to a 3D model or Level-Plot using the EVA-XRD software (Bruker AXS). For SEM images of silica particles one drop of silica sol was dried on the sample holder and no sputtering was used. Pictures were taken with a Zeiss Supra 25.

Results and discussion

Particle characterisation

One important aspect in the use of silica particles in cementitious pastes is the size or rather the size distribution, because it correlates with the particle surface area. Dynamic light scattering (DLS) was used to determine particle sizes in the different solutions. The results are shown in Table 3. The particles have a spherical shape and a narrow size distribution when compared with commercial silica fume, which is shown in Fig. 2.

For the determination of the specific surface of the silica particles different experimental methods are well-established, like nitrogen absorption (BET) or the titration-method of Sears [30], which determines the surface area by absorption of OH^--ions. Assuming a perfect spherical shape of the particles and a silica density of 2.2 g/cm^3 it is also possible to calculate a surface ($Surface_{CALC}$) from the particle diameters determined by dynamic light scattering.

As illustrated in Table 3 there is a large variation in the specific surface area of the silica particles. In general the surface areas calculated from the diameters are smaller than those determined by BET or the Sears method, which suggests, that the particles have a surface roughness or pores. The only exceptions are the smallest particles, where the BET-surface is smaller than expected, which might be caused by agglomeration when the silica sols were dried. In all cases the specific surface area determined by the Sears method is larger than those determined by the BET method.

On the one hand the Sears method has an inaccuracy of ±5% [30]. On the other hand the particles are dispersed instead of being dried and hydroxyl ions may have a better potential to enter pores and gaps in the surface. Even if it is not possible to determine the specific surface more precisely, the results give a good impression about the proportions between the specific surfaces of the different sized particles.

Calorimetry

According to the model by Thomas et al. [29] the surface of the silica particle serves as a nucleation site for the

Table 2 Analysis of cement composition

Oxide	CaO	SiO_2	Al_2O_3	Fe_2O_3	SO_3	MgO	Na_2O	K_2O	L.O.I.
wt%	65.02	21.85	4.48	0.16	2.67	0.67	<0.03	0.82	3.89

Table 3 Particle size (d_{50}) and specific surface area of the silica particles

Solution	Diameter$_{DLS}$ d_{50}, nm	Surface$_{CALC,}$ m^2/g	Surface$_{BET,}$ m^2/g	Surface$_{Sears,}$ m^2/g
Köst 7	7	381	285	409
Köst 14	14	195	240	267
Köst 18	18	152	175	239
Köst 30	71	39	69	76
Solution 1	86	32	65	
Solution 2	246	11	27	
Solution 3	295	9	18	
Silica fume			18–23	

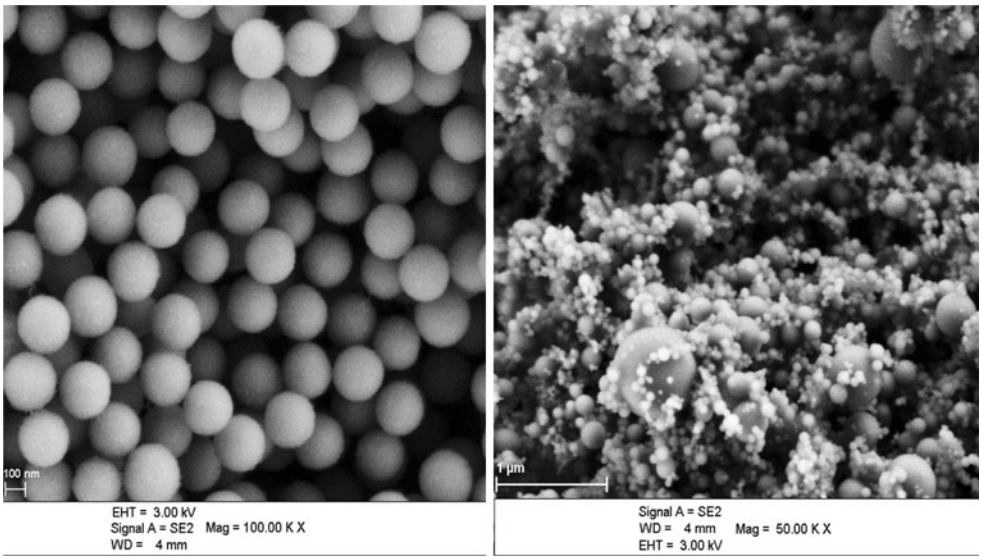

Fig. 2 Silica particles (246 nm) from solution (*left*), silica fume (*right*)

formation of C–S–H-seeds, which cause an acceleration of the hydration process. Hence it follows that there should be a correlation between the total size of the silica particles and the acceleration.

In principle there are two possibilities to control the total surface of the silica particles additive. First, the dosage of the particles in the cement paste can be changed. Secondly the size of the particles can be varied at constant dosage. Both ways will be presented in the following section.

Gartner et al. [31] classified the hydration process into four principle stages. The first stage is the initial phase of just a few minutes which is due to the superficial reaction of C_3S, rapid dissolution of free lime and aluminate phases and the immediate formation of ettringite. This is connected with a high rate of heat evolution which could not be followed in our experiments, since the samples had to be mixed outside the calorimeter. A low rate of hydration heat is characteristic for the following induction period where C–S–H- and portlandite-nucleation begins. For the white cement without additives in our experiments this stage ends approximately one hour after mixing when the acceleration period begins. During this third stage the heat evolution increases significantly, because of rapid hydration of C_3S to form C–S–H-phase and portlandite.

After three hours the reaction gets more and more controlled by diffusion and the heat evolution starts to decrease. In this retardation period a second peak of heat evolution may occur which is related to the formation of sulphate-type-AFm (monosulphate) either by direct tricalcium aluminate (C_3A) hydration with sulphate from pore solution or secondary C_3A hydration with ettringite [32]. In both cases the reaction starts because of an exhaustion of the sulphate carrier and decreasing sulphate concentration in the pore solution. After the formation of the sulphate-type AFm a further decrease of heat evolution follows.

In Fig. 3 particles of 86 nm in diameter were added to the white cement paste. For these particles the time and intensity of the minimum remains unaffected by all added concentrations of silica. In contrast to this, the following maximum of hydration heat increases significantly with increasing concentration of particles in the cement paste. Since the first peak of hydration heat presents the

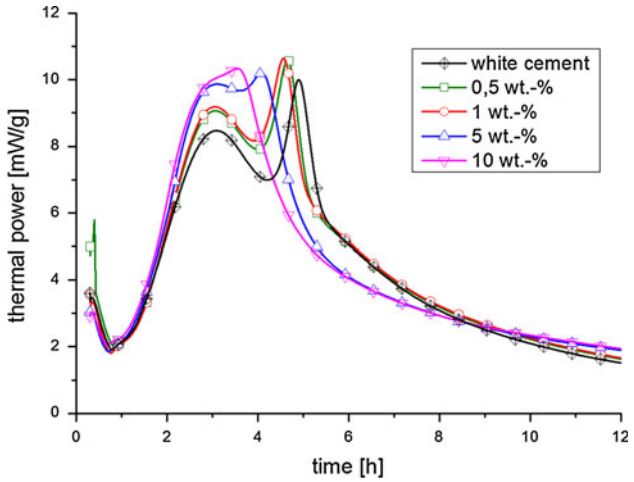

Fig. 3 Calorimetry of cement hydration with admixture of nano-silica of 86 nm in diameter

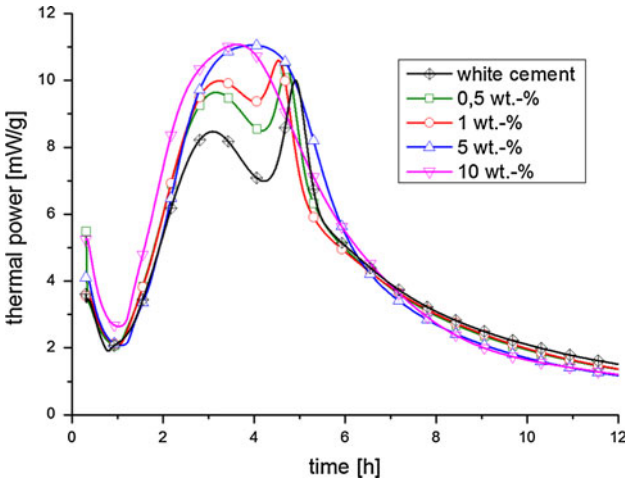

Fig. 4 Calorimetry of cement hydration with admixture of nano-silica of 7 nm in diameter

consumption of C_3S, the formation of $Ca(OH)_2$ and the C–S–H-phase, the hydration rate of C_3S is increased significantly with increasing silica surface. This is in total accordance with our estimation that the acceleration of C_3S hydration should increase because the more the C–S–H-seeds can be formed the larger the total silica surface is.

The second maximum of heat evolution, which is allocated to the formation of sulphate-type AFm-phase, shows a significant shift in time when silica is added to the paste. The larger the silica dosage, the earlier the formation of the monosulphate occurs. Kuzel [32] examined the position of this peak as a function of sulphate concentration in Portland cement. He found that the peak shifts to earlier times the lower the sulphate concentration is. One possible mechanism for the influence of nano-silica on the formation of the sulphate-type AFm is, that the high surface area has a high capacity to adsorb sulphate ions. This decrease in sulphate concentration results in an acceleration of monosulphate formation like Kuzel has found. At the same time the change in sulphate concentration also has an influence on the dissolution and formation of all sulphate containing phases.

If the size of the silica particles is reduced, the effects described before are expected to be even more noticeable as the total silica surface is much larger at the same dosages. This is shown in Fig. 4 for the smallest particles with 7 nm in diameter. The induction period is a little bit longer compared with pure white cement. The first maximum of hydration heat increases significantly with larger silica content in the paste. Even very small amounts of nano-silica result in much higher maximums. At high silica content a further increase of this content from 5 to 10 wt% only minimally increases the maximum heat even though the total silica surface area is doubled. This indicates that there might be an optimum in surface area beyond which the maximum of hydration heat is not increased any more. The second maximum of hydration heat shows a shift to earlier times as seen with the larger particles, even though the shift is stronger here. With high particle content in the paste both peaks merge to a single maximum. This fusion of the peaks was found by Kuzel for Portland cements with sulphate concentrations below 1.87 wt% [32], while our cement has a sulphate concentration of 2.67 wt%. This indicates again, that nano-silica has a large influence on the sulphate equilibrium of the cement paste.

If the total surface size of the particles is not increased by higher concentrations of particles but is increased by using smaller particles a similar effect like in Fig. 4 can be achieved. Figure 5 shows the hydration heat when one mass percent of different sized silica is added. It shows that the height of the first maximum increases with decreasing particle size, even though the mass of silica remains constant. This shows that the acceleration of the cement hydration is not caused by a consumption of the silica but depends just on the particles surface area.

At the same time the second peak of hydration heat, allocated to the formation of sulphate-type AFm, can be obtained at earlier times. Therefore we suggest that smaller particles with large surface areas have larger effects on the behaviour of the sulphate containing phases in the cement paste.

In situ X-ray diffraction

Since the formation of C–S–H-phase plays a crucial role for strength development of cement, there is a special interest to be able to follow it. Due to the fact, that the C–S–H-phases are amorphous for X-ray diffraction, a direct observation of their formation is not possible. However, it is possible to obtain knowledge about this in an indirect way. This can be done by observing the decrease

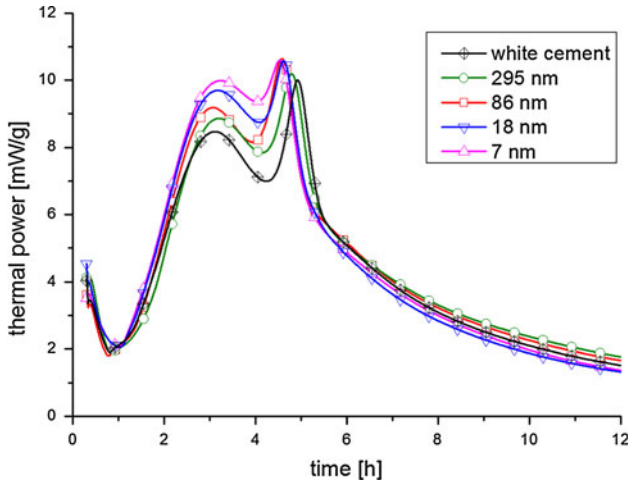

Fig. 5 Calorimetry of cement hydration with admixture of nano-silica of different sizes at 1.0 wt%

of crystalline alite and belite and the increase of portlandite formation by in situ-XRD of hydrating cement paste, as both C–S–H and portlandite are formed simultaneous during the hydration of alite and belite. Level-plots of portlandite formation during the first 24 h of hydration are shown in Fig. 6.

Pure white cement is compared with samples containing 5 wt% silica. The kapton-foil and a water layer between the foil and the cement result in a slight shift of the peaks positions and background noise which varies with the samples' water demand. If the sample sediment, the thickness of the water layer changes and thereby the shift of the peak position continuously changes when sedimentation appears. Therefore only a qualitative description of the results is possible at the moment.

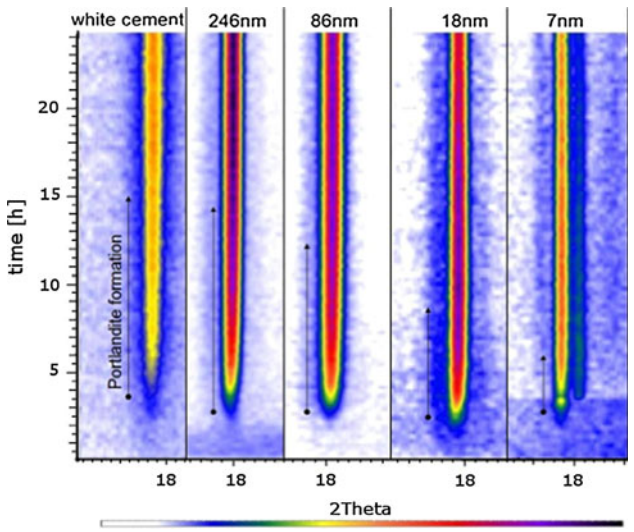

Fig. 6 Level-plots of portlandite during the first 24 h of cement hydration with 10 wt% nano-silica particles added to the cement paste. *Arrows* show the period of time between the beginning of portlandite formation and maximum level

During the hydration of pure white cement the formation of portlandite, which is marked with arrows, starts to increase significantly after 4 h and lasts until 14 h after mixing, when the formation slows down to almost zero. When adding silica particles to the white cement the formation of portlandite slightly shifts to earlier times with decreasing particle size. At the same time there is a strong acceleration of portlandite formation. While the formation of portlandite takes 10 h in pure white cement, this period of time is reduced to 4 h, when the smallest silica particles were added. This shows that the hydration of alite and belite is considerably accelerated due to the admixture of nano-silica. Like we have seen in the calorimetric experiments the acceleration correlates with the total surface area of the added particles, which is approximately 12 times larger for the 7 nm nanosilica then for the 246 nm nanosilica. This is in accordance to our assumption that C–S–H-seeds are formed on the silica surface by an early pozzolanic reaction to accelerate the hydration of C_3S and that this acceleration is more pronounced when large surface areas are present because more C–S–H-seeds can be formed.

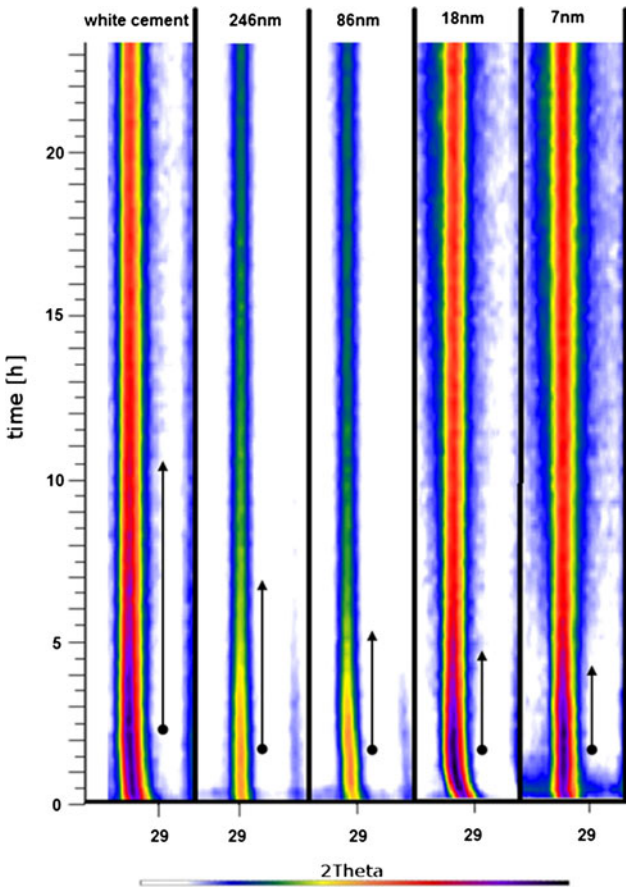

Fig. 7 Level-plot of C_3S during the first 24 h of cement hydration with 10 wt% nano-silica added to the cement paste. The period of time of rapid C_3S consumption is marked with *arrows*

In Fig. 7 the consumption of C_3S is shown for the first 24 h with the Addition of 10 wt% nano-silica. The time interval of rapid C_3S consumption is marked with arrows. A significant shortening of this period can be obtained, when nano-silica is added and it directly correlates with the total surface area of the particles. The consumption of C_3S occurs at the same time as the first maximum of heat evolution. Combined with the information of Fig. 5 that the height of the maximum increases when silica is added, the period of C_3S hydration can be characterised as shorter and more intense when silica is added and therefore is a real acceleration of C_3S hydration.

A faster formation of portlandite and faster consumption of C_3S suggests that the formation of C–S–H-phase is accelerated as well. Since the C–S–H-phase is the main component for strength development in cement, this acceleration should result in higher early strength of the hardened cement pastes, which will be illustrated in another publication.

Conclusions

When nano-silica is added to ordinary Portland cement, the hydration heat in the main period increases significantly with increasing silica surfaces. This is attended by a faster formation of portlandite and a faster consumption of C_3S during the first hours after mixing. Both results together show that C_3S hydration is accelerated by nano-silica addition. In all cases the acceleration was controlled by the total surface area of the added silica particles. Our assumption that the acceleration is caused by C–S–H-seeds that are formed on the silica surface and that the acceleration therefore should be dependent on the surface area was confirmed by all experiments.

At the same time the formation of sulphate-type AFm was obtained much earlier when nano-silica was added. Because the point of time of the sulphate-type AFm formation depends on the sulphate concentration in the cement paste we suggest that nano-silica has a major role in the reactions of the sulphate containing phases during cement hydration. A possible mechanism is the ability of the large silica surface area to adsorb ions from the solution and thereby change the specific sulphate equilibrium in the solution.

Acknowledgements The Authors want to thank Prof. Dr. A. Kwade, Dr. S. Breitung-Faes (both TU Braunschweig) and Dr. C. Gellermann (Fraunhofer ISC) for DLS measurements and SEM image.

References

1. Iler RK (1979) The chemistry of silica—solubility, polymerization, colloid and surface properties, and biochemistry. Wiley-Interscience, New York
2. Flörke OW, Martin B, Benda L, Paschen S, Bergna HE, Roberts WI, Welsh WA, Ettlinger M, Kerner D, Kleinschmit P, Meyer J, Gies H, Schiffmann D (2005) Silica. Ullmann's encyclopedia of industrial chemistry, vol VA23. VCH Publishers Inc., Weinheim, p 1
3. Stöber W, Fink A, Bohn E (1968) J Colloid Interf Sci 26:62
4. Nozawa K, Gailhanou H, Raison L, Panizza P, Ushiki H, Sellier E, Delville JP, Delville MH (2005) Langmuir 21(4):1516. doi:10.1021/La048569r
5. Nishimori H, Tatsumisago M, Minami T (1997) J Sol-Gel Sci Technol 9(1):25
6. Graf C, Vossen DLJ, Imhof A, van Blaaderen A (2003) Langmuir 19(17):6693
7. Dorcheh AS, Abbasi MH (2008) J Mater Process Technol 199(1–3):10. doi:10.1016/j.jmatprotec.2007.10.060
8. Jonckbloedt RCL (1998) J Geochem Explor 62(1–3):337
9. Lieftink DJ, Geus JW (1998) J Geochem Explor 62(1–3):347
10. Estevez M, Vargas S, Castano VM, Rodriguez R (2009) J Non-Cryst Solids 355(14–15):844
11. Korpa A, Trettin R, Bottger KG, Thieme J, Schmidt C (2008) Adv Cem Res 20(1):35. doi:10.1680/ader.2008.20.1.35
12. Schmidt M, Stephan D, Krelaus R, Geisenhanslüke C (2007) Cem Int 5(4):86
13. Teichmann T, Schmidt M (2004) In: Schmidt M, Fehling E, Geisenhanslüke C (eds) Ultra high performance concrete (UHPC). Kassel university press, Kassel, p 313
14. Korpa A, Trettin R (2004) In: Schmidt M, Fehling E, Geisenhanslüke C (eds) Ultra high performance concrete (UHPC), GmbH, Kassel, p 155
15. Schmidt M, Stephan D, Krelaus R, Geisenhanslüke C (2007) Cem Int 5(6):72
16. Benezet JC, Benhassaine A (1999) Powder Technol 105(1–3):167
17. Benezet JC, Benhassaine A (1999) Powder Technol 103(1):26
18. Chandra S, Bergqvist H (1997) In: Paper presented at the proceedings of the 10th international congress chemistry of cement, Goeteborg, Sweden
19. Korpa A, Trettin R (2007) Cem Int 5(1):74
20. Jo B-W, Kim C-H, Tae G-h, Park J-B (2007) Constr Build Mater 21:1351
21. Porro A, Dolado JS, Campillo I, Erkizia E, Miguel Yd, Saez de Ibarra Y, Ayuela A (2005) In: Ravindra D (ed) Application of nanotechnology in concrete design. Telford, p 87
22. Qing Y, Zenan Z, Deyu K, Rongshen C (2007) Constr Build Mater. doi:10.1016/j.conbuildmat.2005.1009.1001
23. Shih JY, Chang TP, Hsiao TC (2006) Mat Sci Eng a-Struct 424(1–2):266
24. Tobón JI, Restrepo OJ, Borrachero MV, Payá J (2011) In: 13th international congress on the chemistry of cement, Madrid
25. Harsh S, Arora AK, Ali MM, Vasudeva M (2011) In: 13th international congress on the chemistry of cement, Madrid
26. Björnström J, Martinelli A, Matic A, Börjesson L, Panas I (2004) Chem Phys Lett 392(1–3):242
27. Collodetti G, Repette WL, Hotza D, Gleize PJP (2011) In: 13th international congress on the chemistry of cement, Madrid
28. Ji T (2005) Cem Concr Res 35(10):1943
29. Thomas JJ, Jennings HM, Chen JJ (2009) J Phys Chem C 113(11):4327. doi:10.1021/jp809811w
30. Sears GW (1956) Anal Chem 28(12):1981
31. Gartner EM, Young JF, Damidot DA, Jawed I (2002) In: Bensted J, Barnes P (eds) Structure and performance of cements. Spon Press, London, p 57
32. Kuzel HJ (1994) In: 16th international conference on cement microscopy, Richmond, VA, USA, p 125